Synthesis and Characterization of Colorless Polyimide Nanocomposite Films

Chul Ha Ju,[1] Jeong-Cheol Kim,[2] Jin-Hae Chang[1]

[1]*Department of Polymer Science and Engineering, Kumoh National Institute of Technology, Gumi 730-701, Korea*
[2]*Gwangju R&D Center, Korea Institute of Industrial Technology, Gwangju, 500-460, Korea*

Received 18 March 2007; accepted 3 June 2007
DOI 10.1002/app.26987
Published online 7 September 2007 in Wiley InterScience (www.interscience.wiley.com).

ABSTRACT: A poly(amic acid) was prepared through the reaction of 4,4′-(hexafluoroisopropylidene)diphthalic anhydride and 2,2′-bis(trifluoromethyl) benzidine in *N,N*-dimethylacetamide. Hybrid films were obtained from blend solutions of the precursor polymer and the organoclay dodecyltriphenylphosphonium–mica, with the organoclay content varying from 0 to 1.0 wt %. The cast films of poly(amic acid) were heat-treated at different temperatures to create polyimide (PI) hybrid films. These PI hybrid films showed excellent optical transparency and were almost colorless. The intercalation of PI chains in the organoclay was examined with wide-angle X-ray diffraction and electron microscopy. In addition, the thermomechanical properties were tested with differential scanning calorimetry and thermogravimetric analysis, and the gas permeability was determined. The addition of only a small amount of the organoclay was sufficient to improve the thermal and mechanical properties of the PI, with the maximum enhancement being observed with 0.5 wt % organoclay. However, the water vapor permeability decreased with the clay loading increasing from 0 to 0.5 wt %. © 2007 Wiley Periodicals, Inc. J Appl Polym Sci 106: 4192–4201, 2007

Key words: films; nanocomposites; nanotechnology; organoclay; polyimides

INTRODUCTION

The outstanding thermal, mechanical, and electrical properties of aromatic polyimides (PIs), as well as their resistance to solvents, have led to their use as interlayer dielectrics in semiconductor devices, wire-coating materials, and substrates for flexible printed circuits.[1–3] In general, however, PIs are difficult to process on account of their nonmelting behavior and poor solubility in conventional organic solvents. As a result, PIs can be used only in certain applications.[4,5]

Much research has been devoted to developing high-performance PI materials with excellent thermomechanical properties, good solubility, and optical transparency.[6–9] For example, PIs containing trifluoromethyl groups have been synthesized that show a high modulus, a low thermal expansion coefficient, and good solubility in conventional organic solvents, and the incorporation of heterocyclic units into PI chains has been found to increase the glass-transition temperature (T_g) and thermooxidative stability.[10–12] Transparent PIs have been prepared with dianhydride and diamine monomers substituted with fluorine moieties in the side groups.[13,14] Moreover, these colorless PIs have superior solubility, thermal stability, and optical transparency characteristics in comparison with other commercialized PIs; however, these colorless PIs also exhibit reduced moisture absorption and color intensity. Optically transparent PI films have many potential uses in electro-optical devices and semiconductor applications. Recently, Yang and coworkers[13,14] prepared a series of soluble and light-colored PIs, which bore fluorinated pendant groups on the heterocyclic imide main chain, through the solution condensation of aromatic dianhydrides and aromatic diamines. In that work, they found a systematic relationship between the structure and coloration.

Organic–inorganic nanometer-scale blended composites, called nanocomposites or organic–inorganic hybrids, have attracted great interest because of their unexpected hybrid properties synergistically derived from the two components.[15,16] Organic–inorganic hybrids with excellent thermomechanical and gas-barrier properties and with inorganic contents that are much lower than those in conventionally filled polymer composites have been prepared. Moreover, it has been found that the higher the degree of delamination is in polymer/clay nanocomposites, the greater the enhancement is of these properties.[17–19]

Correspondence to: J.-H. Chang (changjinhae@hanmail. net).
Contract grant sponsor: Program for the Training of Graduate Students in Regional Innovation (Ministry of Commerce, Industry, and Energy of the Korean Government).

Even at low clay concentrations (<10 wt %), the strength and initial modulus can be substantially increased compared with those of the pure polymer, whereas the gas permeability is reduced by the planar orientation of the clay sheets. Clays have sandwich-type structures that typically consist of one octahedral Al sheet and two tetrahedral Si sheets, a so-called philosilicate structure. There are many types of philosilicates: kaolinite, montmorillonite, hectorite, saponite, synthetic mica, and so on. Previously, we used[20] dodecylamine and hexadecylamine as aliphatic alkylamines to prepare organomontmorillonites in a PI matrix, and we characterized their thermal and mechanical properties as well as their gas permeabilities and morphologies.

In this study, we prepared nanocomposite films composed of a PI and an organoclay and examined their properties as a function of the organoclay content. The colorless PI was synthesized by the thermal cyclization of an aromatic precursor polymer bearing trifluoromethyl-substituted benzene in the side groups. Our approach is based on the reaction of 4,4′-(hexafluoroisopropylidene) diphthalic anhydride (6FDA) and 2,2′-bis(trifluoromethyl) benzidine (TFB), which are monomers of a colorless PI. To obtain nanocomposites without producing thermal degradation during processing, we used a thermally stable organoclay. Films of the nanocomposites with various organoclay contents were prepared with a solution intercalation method, and their morphologies and thermomechanical and optical properties were determined.

EXPERIMENTAL

Materials

Na^+-type fluorinated synthetic mica (Na^+–mica), with the free OH group of the mica replaced by fluorine, was supplied by CO-OP, Ltd. (Tokyo, Japan). Mica consists of stacked silicate sheets with a length of about 1230 nm and a thickness of about 1 nm. The cationic exchange capacity of Na^+–mica was found to be 70–80 mequiv/100 g. All reagents were purchased from TCI (Tokyo, Japan) and Aldrich Chemical Co. (Seoul, Korea). 6FDA and TFB were obtained from TCI and were used as received. *N*,*N*-dimethylacetamide (DMAc) was purified and dried over molecular sieves before use. All other reagents were used without further purification.

Preparation of the organoclay and colorless PI hybrid films

The organically modified mica used in this study was synthesized with an ion-exchange reaction between Na^+–mica and dodecyl triphenylphosphonium chloride ($C_{12}PPh–Cl^-$). The resulting organically modified mica, dodecyltriphenylphosphonium–mica ($C_{12}PPh$–mica), was obtained through a multistep route.[21]

Poly(amic acid) (PAA) was synthesized from 6FDA and TFB in DMAc by the low-temperature method.[22] TFB (6.5 g, 2.0×10^{-2} mol) and DMAc (40 mL) were placed in a 100-mL, three-necked flask, and the mixture was stirred at 0°C for 30 min under a nitrogen atmosphere. 6FDA (9.0 g, 2.0×10^{-2} mol) in DMAc (50 mL) was then added. The resulting solution was stirred vigorously at 0°C for 1 h and then at room temperature for 12 h, yielding a 15 wt % DMAc solution of PAA.

Because the synthetic procedures used to produce the polymer/organoclay nanocomposites were the same for all $C_{12}PPh$–mica contents, here we only describe the preparation of PI/$C_{12}PPh$–mica (0.50 wt %) as a representative example. A dispersion of 0.074 g of $C_{12}PPh$–mica, 14.9 g of a PAA solution, and excess DMAc (30 mL) was stirred vigorously at room temperature for 24 h. The solution was cast onto glass plates, and then the solvent was evaporated in a vacuum oven at 50°C for 2 h. To remove the solvent, the film was subjected to ultrasonication three times for 5 min each. After the solvent had been removed, the film was dried again in a vacuum oven at 30°C for 2 h. The film thickness was 60–90 μm. The PAA film was further imidized on the glass plate by sequential heating at 110, 140, 170, 195, and 220°C for 30 min at each temperature followed by 2 h at 230°C.

IR (film): 1779 and 1725 (imide C=O), 1619–1481 (aromatic C=C stretch), 1378 (C—N stretch), 1240 (C—O), 1100–1300 cm^{-1} (C—O and C—F stretching).

No fixed tools were used for orientation on the glass plate during heat treatment because orientation can influence some characteristics of film specimens, such as the tensile properties and morphology. The chemical structures along the synthetic route are shown in Scheme 1.

Characterization

Wide-angle X-ray diffraction (XRD) measurements were performed at room temperature on a Rigaku D/Max-IIIB X-ray diffractometer (Tokyo, Japan) with Ni-filtered Cu Kα radiation. The scan rate was 2°/min over a range of $2\theta = 2–25°$. Differential scanning calorimetry (DSC) and thermogravimetric analysis (TGA) were performed on a DuPont 910 instrument at a heating rate of 20°C/min.

The tensile properties of the solution-cast films were determined with an Instron model 5564 universal testing machine (MA) at a crosshead speed of 2 mm/min. The specimens were prepared by the cutting of strips with dimensions of 5×70 mm^2. The

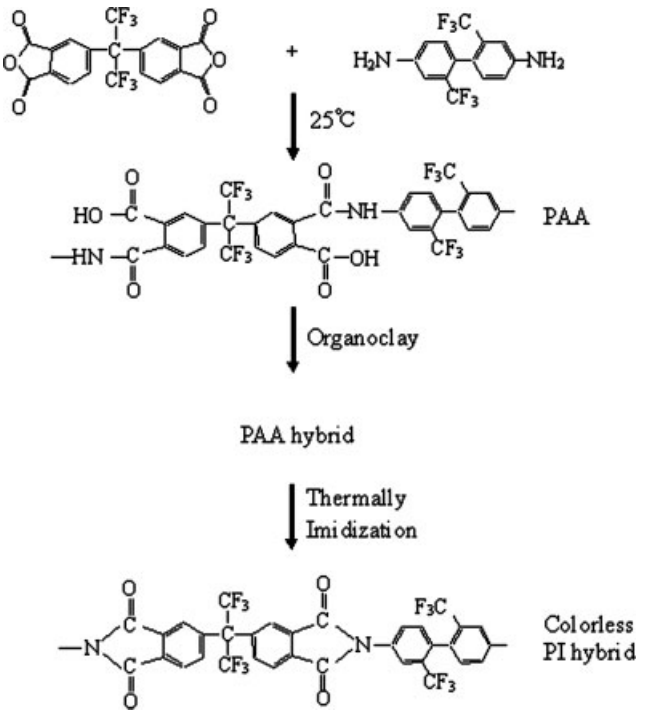

Scheme 1 Synthetic scheme for the colorless PI nanocomposite.

reported data represent the mean of at least 10 individual determinations. The experimental uncertainties in the tensile strength and modulus were ±1 MPa and ±0.05 GPa, respectively.

The water vapor permeability was measured according to ASTM E 96 with a MOCON model DL 100 data logger. The values of the water vapor transmission rate were obtained at 38°C.

The morphologies of the fractured surfaces of the extrusion samples were investigated with a Hitachi S-2400 scanning electron microscope (Tokyo, Japan). To enhance the conductivity, the fractured surfaces were sputter-coated with gold with an SPI sputter coater (Tokyo, Japan). Transmission electron microscopy (TEM) micrographs of ultrathin sections of the PI/C_{12}PPh–mica hybrid films were recorded with an EM 912 Omega transmission electron microscope with an acceleration voltage of 120 kV.

The color intensity of the polymer films was evaluated with a Minolta model CM-3500d spectrophotometer (Tokyo, Japan). The measurements were taken with films 60–90 μm thick. Ultraviolet–visible (UV–vis) spectra of the polymer films were recorded on a Shimadzu UV-1601 UV–vis spectrophotometer (Tokyo, Japan).

RESULTS AND DISCUSSION

Optical properties

Optical nanocomposite materials must scatter light only to a small extent to achieve high transparency and optical purity. To minimize light scattering, the dispersed phase should have an average size that is below the wavelength range of visible light (i.e., <400 nm).[23] Hence, the synthesis of polymeric nanocomposites, although more difficult than the fabrication of traditional composites, does not pose serious problems when the material is destined for optical applications.

Recently, fluorinated PIs were synthesized with a diamine bearing pendant CF_3 groups and commercial aromatic dianhydrides.[24–26] One such dianhydride, based on 6FDA, was used to form a PI that was much lighter in color than commercially available Kapton, which is based on pyromellitic dianhydride and oxydianiline. The organoclay/PI hybrid films prepared in this work were almost colorless and became less transparent as the organoclay content was increased from 0.25 to 1.00 wt % (Table I). The optical properties of Kapton are also shown in Table I for reference.

The b^* value of the PI hybrid with 0.25 wt % organoclay was 1.68, and its degree of colorlessness was almost the same as that of aliphatic poly(methyl methacrylate) ($b^* = 1.2$).[14] The value of b^*, however, increased from 3.03 to 3.39 as the organoclay content increased from 0.50 to 1.00 wt % because of the agglomeration of the clay particles. This increase in b^* suggests that the organoclay particles were better dispersed in the polymer matrix at lower organoclay loadings.

The solvent-cast hybrid films with organoclay contents in the range of 0–1.0 wt % were all almost colorless, as shown in Figure 1(a–e), and this indicated that the addition of the organoclay to the PI matrix did not significantly affect the transparency. Compared with the 0.25–0.75 wt % hybrid films, the film containing 1.00 wt % organoclay did, however, have a more yellowish color [see Fig. 1 (e)], although it was still sufficiently transparent for optical applications. These findings suggest that, even at an organoclay loading of 1.0 wt %, the phase domains in the

TABLE I
Color Coordinates of the PI Nanocomposite Films

Organoclay (wt %)	Film thickness (μm)	L^*[a]	a^*[b]	b^*[c]
Kapton 200KN	50	65.50	12.27	44.69
0 (pure PI)	79	90.69	−1.38	1.17
0.25	81	89.75	−1.29	1.68
0.50	80	89.44	−1.52	3.03
0.75	89	89.23	−1.47	3.39
1.00	62	87.90	−1.29	3.22

[a] 100 is white, and 0 is black.
[b] A positive value indicates red, and a negative value indicates green.
[c] A positive value indicates yellow, and a negative value indicates blue.

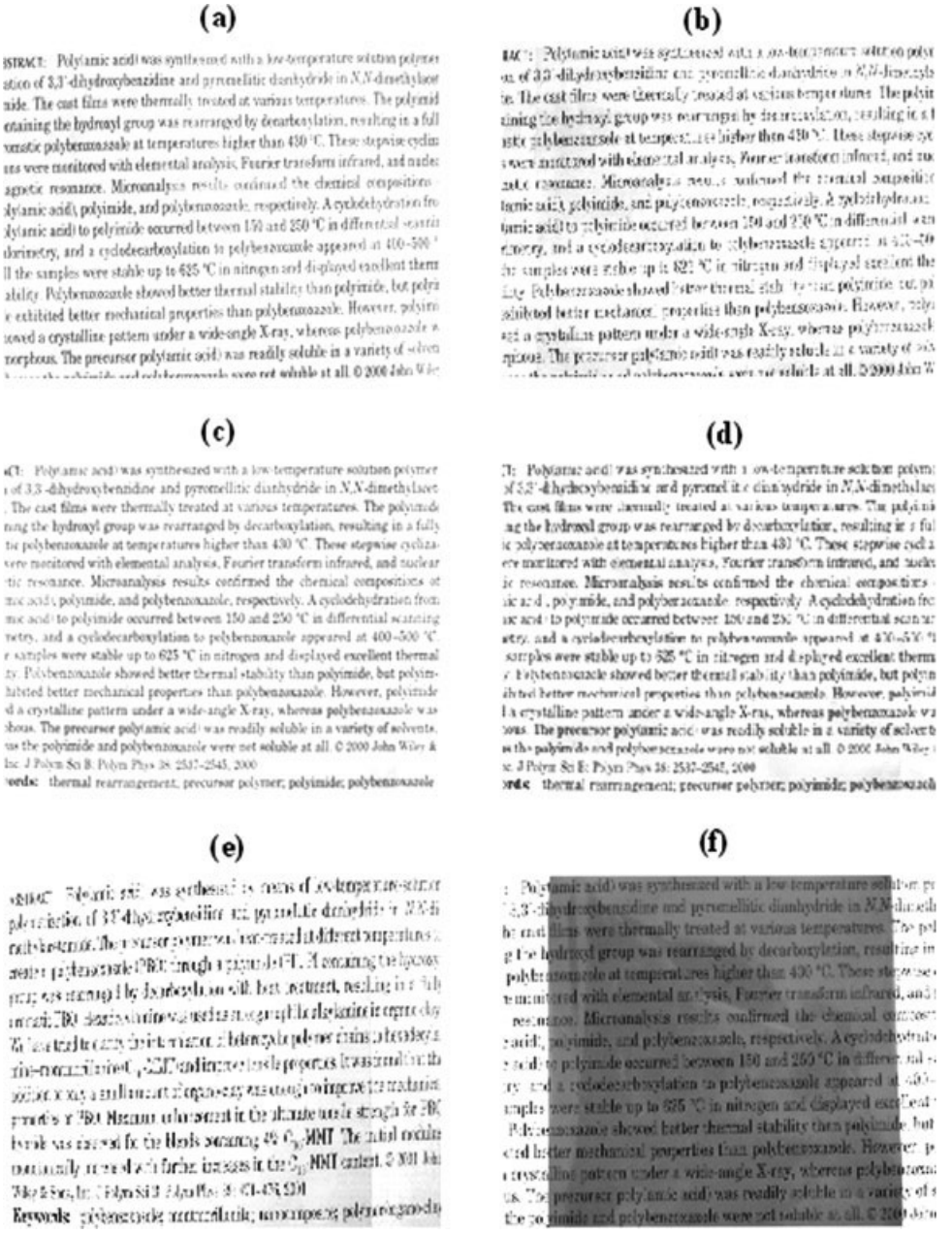

Figure 1 Photographs of PI/organoclay hybrid films containing (a) 0 (pure PI), (b) 0.25, (c) 0.50, (d) 0.75, or (e) 1.0 wt % C_{12}PPh–mica. (f) Kapton 200KN is shown as a reference.

hybrid film were predominantly smaller than the wavelength range of visible light.[23,27] Thus, the hybrid films prepared in this work exhibited excellent transparency because of a high dispersion of clay particles in the polymer matrix, although the transparency diminished slightly with increasing organoclay content because of the agglomeration of the clay particles.

The color intensities of the hybrid films could be elucidated from the cutoff wavelength (λ_0) observed in the UV–vis absorption spectra. The UV–vis spectra of the PI hybrid films with organoclay contents ranging from 0 to 1.00 wt % are shown in Figure 2. The PI hybrid films containing 0 (pure PI) and 0.25 wt % C_{12}PPh–mica showed the highest transmittance and lowest λ_0 values among the hybrid films. The low λ_0 value and colorless nature of the pure PI film could be attributed to the CF_3 groups in the monomers, which inhibited charge-transfer complex formation and decreased intermolecular interactions.[13,14] In addition, the superior transparency of the PI films containing 0 or 0.25 wt % C_{12}PPh–mica could be attributed to the limited electronic conjugation along the backbone of these 6FDA-based PIs.[25,28] As the organoclay content was increased above 0.25 wt %, however, λ_0 increased linearly with

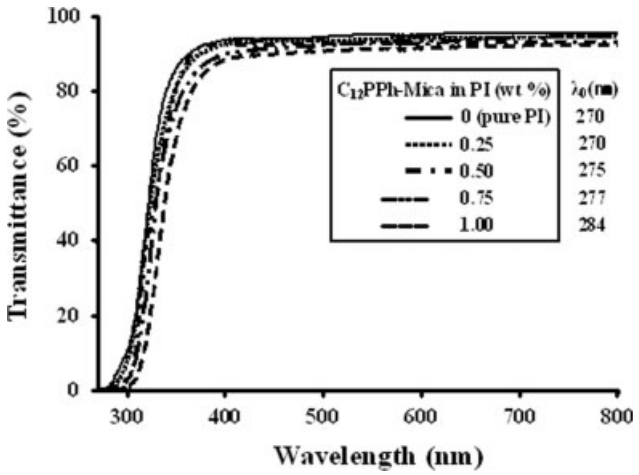

Figure 2 UV–vis transmittance (%) of PI hybrid films with various organoclay contents.

increasing organoclay content because of the agglomeration of the clay particles. Specifically, λ_0 increased from 275 to 284 nm as the C_{12}PPh–mica content increased from 0.50 to 1.00 wt %. Evidence of clay agglomeration obtained with XRD and scanning electron microscopy (SEM) is presented later (Figs. 3 and 4). These colorless PI films showed UV transmittance above 90% at 450 nm and excellent optical properties with a value under a yellow index of 7.

Organoclay dispersion

Figure 3 shows the XRD patterns of the pristine clay and organoclay and those of PI hybrid films with organoclay loadings ranging from 0.25 to 1.00 wt %. The d_{001} reflection for Na^+–mica was observed at $2\theta = 9.23^\circ$, which corresponded to an interlayer distance of 9.57 Å. The XRD peak for the surface-modified clay, C_{12}PPh–mica, was observed at $2\theta = 3.19^\circ$, which corresponded to an interlayer distance of 27.63 Å. As expected, the ion exchange between Na^+–mica and $C_{12}PPh–Cl^-$ resulted in an increase in the basal interlayer spacing compared with that of pristine Na^+–mica, which manifested as a large shift in the diffraction peak toward lower values of 2θ. This increase in the interlayer spacing also led to easier dissociation of the clay, resulting in hybrids with better clay dispersion.[29,30]

In the XRD curves of the pure PI and PI hybrid films in Figure 3, the films containing 0–1.00 wt % organoclay all exhibit a very small diffraction peak at $2\theta = 6.63^\circ$ (d = 13.30 Å) compared with the diffraction peak at $2\theta = 3.19^\circ$ (d = 27.63 Å) for C_{12}PPh–mica. The appearance of a peak at this value of 2θ indicates the possible presence of partially intercalated layers of organoclay dispersed in the PI. The shift in the d-spacing of the C_{12}PPh–mica layers after imidization (27.63–13.30 Å) can be explained by the fact that PAA molecules outside the mica layers squeeze the clay layers during the solvent removal process in the imidization step, causing a reduction in the spacing between the clay layers.[31] This squeezing mechanism should also serve to inhibit exfoliation of the organoclay in the PI, causing the organoclay to exist in the form of an intercalated layer structure. However, although XRD data are very useful for determining the d-spacing of ordered immiscible or intercalated polymer nanocomposites, they may be inadequate for analyzing disordered and exfoliated materials. The dispersion of clay particles in the PI matrix was therefore further examined with electron microscopy, which provided data that complemented the information that could be extracted with XRD.[17,32,33]

Morphology

The morphologies of the PI films containing up to 1.00 wt % C_{12}PPh–mica were examined by the observation of their fracture surfaces with SEM (Fig. 4). Figure 4(b–e) shows clay phases within the hybrid films with organoclay contents of 0.25–1.00 wt %. The PI hybrid films containing 0.25 or 0.50 wt % C_{12}PPh–mica contained clay domains 40–50 nm in size that were well dispersed in a continuous PI phase [Fig. 4(b,c)]. In contrast, the 0.75 wt % C_{12}PPh–mica/PI hybrid film [Fig. 4(d)] contained clay phases with diameters of 250–350 nm dispersed in a continuous PI phase. The micrograph of the 1.00 wt % C_{12}PPh–mica/PI hybrid film [Fig. 4(e)], however, shows voids and some deformed regions that can be attributed to the coarseness of the fractured surface. A comparison of the micrographs reveals that the fractured surfaces of the hybrid films with higher clay contents were more deformed than those

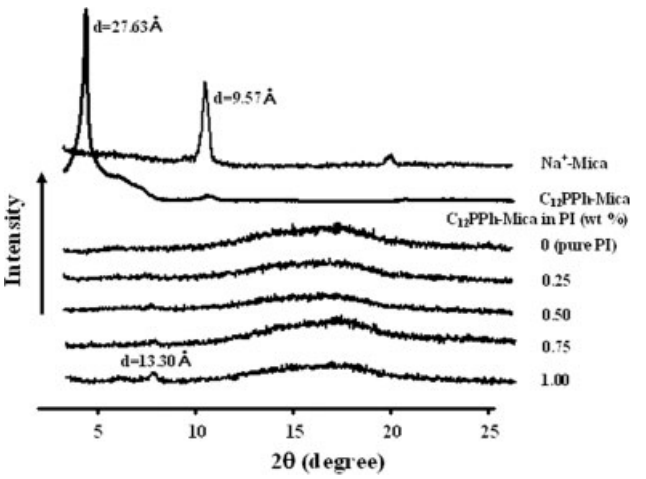

Figure 3 XRD patterns of Na^+–mica, C_{12}PPh–mica, and PI hybrids with various organoclay contents.

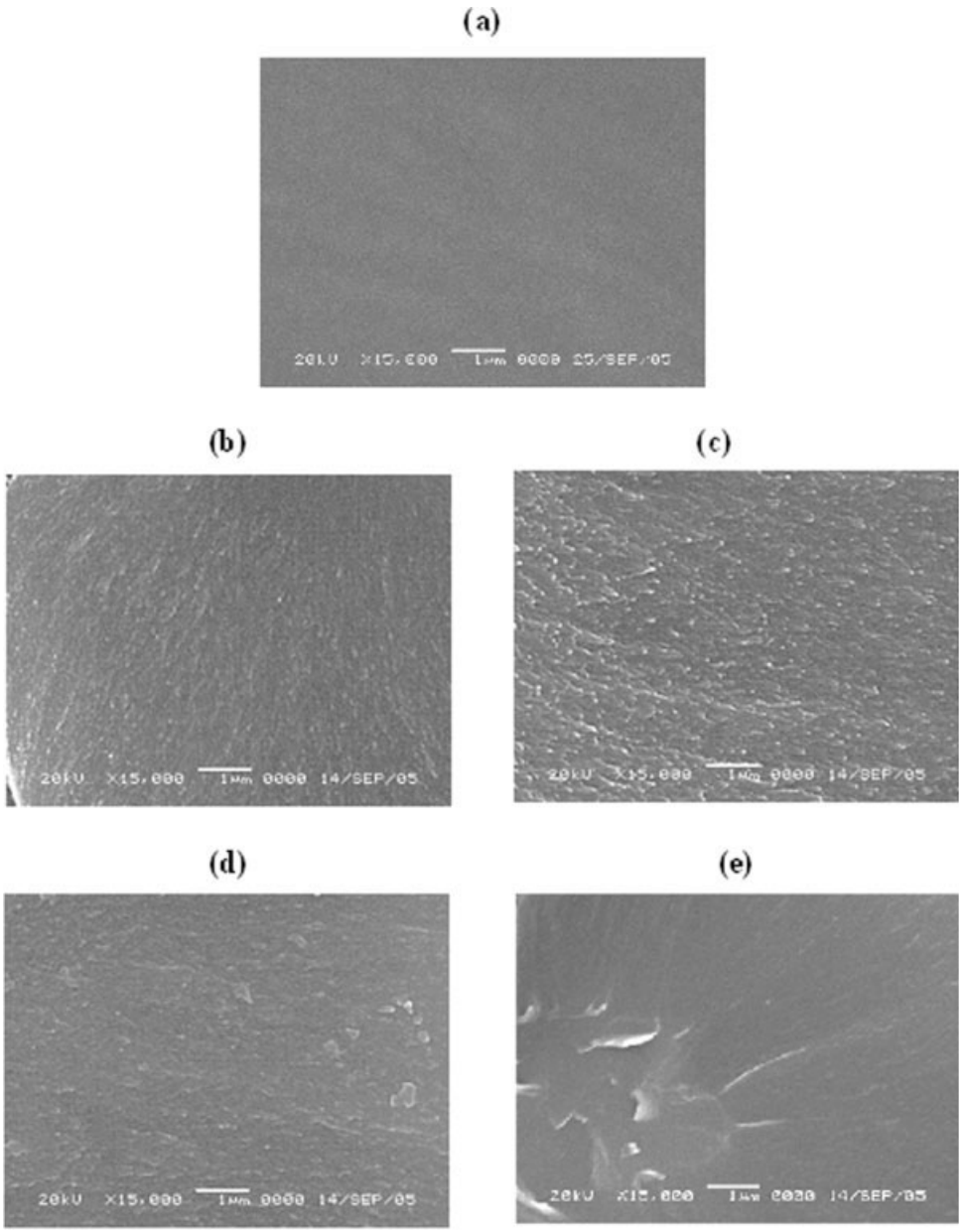

Figure 4 SEM micrographs of PI/organoclay hybrids containing (a) 0 (pure PI), (b) 0.25, (c) 0.50, (d) 0.75, or (e) 1.0 wt % C_{12}PPh–mica.

of the films with low clay contents, likely because of the agglomeration of clay particles. This hypothesis is supported by the observation of agglomerated clay particles in the PI hybrid films with clay contents of 0.75 and 1.00 wt %.

More direct evidence for the formation of a true nanoscale composite was provided by a TEM analysis of ultramicrotomed sections of the hybrid films. TEM micrographs of the 0.50 wt % hybrid film taken at different magnifications are shown in Figure 5. In these images, the dark lines correspond to the intersections of 1-nm-thick sheet layers. The TEM micrographs show that the organoclay was dispersed in the polymer matrix at all magnification levels, although some clay agglomerates with sizes greater than approximately 20 nm can be observed, indicating that nanocomposites formed. These findings thus indicate that during the solution intercalation polymerization, mica was broken down into nanoscale building blocks and dispersed homogeneously in the polymer matrix to afford polymer/clay nanocomposites.

Thermal behaviors

The thermal properties of the PI hybrids with various organoclay contents are listed in Table II. The PIs were soluble in DMAc, which was used in the

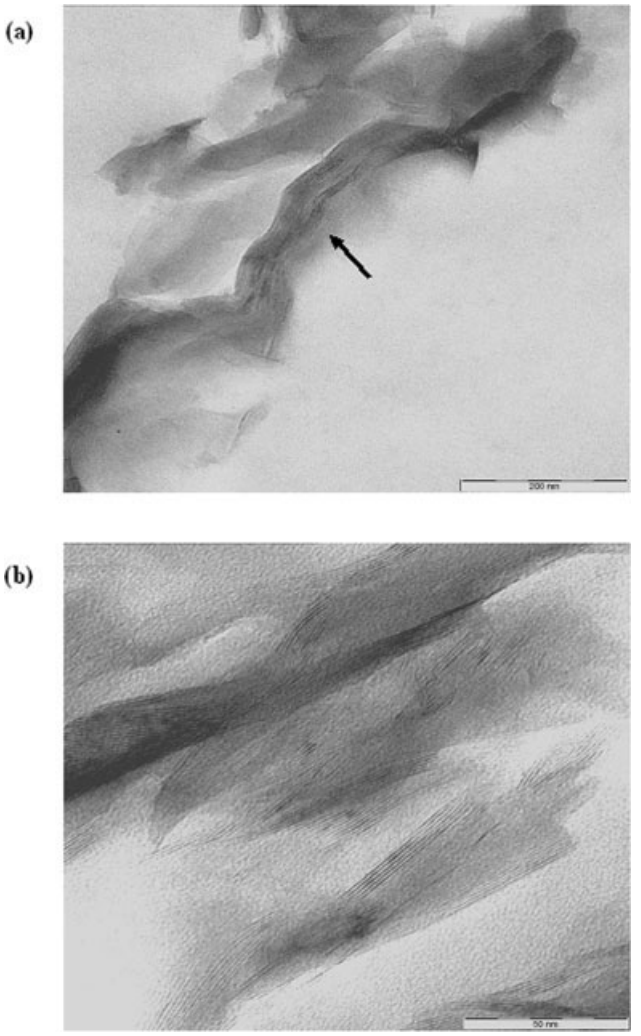

Figure 5 TEM micrographs of PI hybrid films with 0.5 wt % C_{12}PPh–mica. The magnification level increases from micrograph a to micrograph b.

measurement of the solution viscosity. The inherent solution viscosities of the PI hybrid films ranged from 0.57 to 0.60 dL/g (see Table II).

The T_g values of the PI hybrid films increased linearly from 276 to 282°C as the clay loading was increased from 0 to 0.50 wt %. The increase in T_g of these hybrids with an increasing clay loading was likely due to two factors:[34] (1) the significant effect of small amounts of dispersed clay layers on the free volume of the PI and (2) the confinement of intercalated polymer chains within the clay galleries, which prevented the segmental motions of the chains. Similar results have been obtained in other studies of polymer nanocomposites.[35,36] The DSC results for the pure PI and PI hybrid films with 0–1.00 wt % C_{12}PPh–mica are shown in Figure 6.

The initial thermal degradation temperature ($T_D{}^i$) values of the PI hybrid films were also found to

TABLE II
Thermal Properties of the PI Nanocomposite Films

Organoclay (wt %)	Inherent viscosity[a]	T_g (°C)	$T_D{}^i$[b] (°C)	Residue at 900°C (wt %)
0 (pure PI)	0.57	276	480	50
0.25	0.57	278	489	50
0.50	0.59	282	512	50
0.75	0.59	280	498	50
1.00	0.60	278	496	51

[a] Measured at 30°C with 0.1 g/100 mL solutions in DMAc.
[b] Initial 2% weight loss temperature.

increase linearly from 480 to 512°C as the organoclay loading was increased from 0 to 0.50 wt % (see Table II). The increase in the initial decomposition temperature with increasing clay content could be attributed to the fact that the clay acted as a superior insulator and as a mass-transport barrier to the volatile products generated during decomposition.[34,37] Moreover, the clay-induced increase in the thermal stability could also be attributed to the high thermal stability of the clay and to the interactions between the clay particles and the polymer matrix. The TGA curves for the clay, organoclay, and PI hybrid films with various organoclay contents are shown in Figure 7.

In contrast to the behavior observed for organoclay contents of 0–0.50 wt %, the T_g and $T_D{}^i$ values of the hybrids decreased with the organoclay content increasing from 0.50 to 1.00 wt %. For example, the T_g and $T_D{}^i$ values of the PI hybrid films with a 1.00 wt % clay loading were lower by 4 and 16°C, respectively, compared with those of the PI hybrid containing 0.50 wt % organoclay. This decrease in T_g and $T_D{}^i$ seems to be the result of clay agglomeration, which occurs when the clay content in the polymer matrix exceeds some critical value.[36,38,39] In contrast to the thermal properties, the weight of the residue

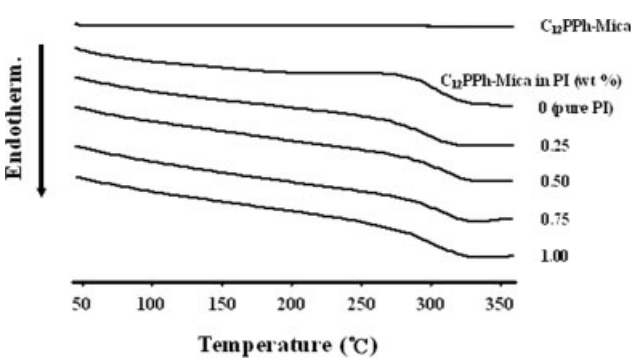

Figure 6 DSC thermograms of C_{12}PPh–mica and PI hybrids with various organoclay contents.

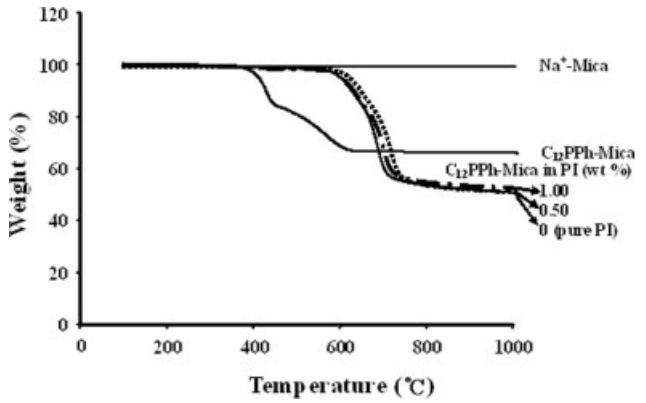

Figure 7 TGA thermograms of Na^+–mica, C_{12}PPh–mica, and PI hybrids with various organoclay contents.

at 900°C remained fairly constant as the clay loading varied from 0 to 1.00 wt %, as shown in Table II.

Mechanical properties

The tensile mechanical properties of the PI and hybrid films are given in Table III. The ultimate tensile strength increased linearly with increasing organoclay content up to 0.50 wt %, at which it had a value 1.2 times that of pure PI. Upon a further increase in the organoclay content above 0.50 wt %, however, the ultimate tensile strength decreased markedly. This drop-off in strength at organoclay contents above 0.50 wt % could be explained by agglomeration of the C_{12}PPh–mica domains, a hypothesis that is supported by the XRD and SEM data presented previously. Similar trends were also observed for the thermal properties of the hybrid films (Table II).

The initial tensile modulus of the C_{12}PPh–mica hybrid films also increased with the addition of clay up to a critical content and then decreased above that critical loading. The 0.50 wt % PI hybrid exhibited the highest value of the modulus, 3.89 GPa, which was about 40% higher than that of pure PI (2.78 GPa). This enhancement of the modulus was ascribed to the high resistance exerted by the clay. Furthermore, the increased stretching resistance of the polymer chains produced by the orientation of their backbones in the galleries also contributed to the enhancement of the modulus. The observed increase in the initial tensile modulus upon the addition of up to 0.50 wt % organoclay to the PI film was consistent with previous reports that regions in a polymer/clay hybrid in which the polymer chain mobility is restricted make significant contributions to the tensile modulus of the hybrid.[40,41] When, however, the organoclay content reached 1.00 wt %, the modulus decreased to 2.87 GPa. This decrease in the initial tensile modulus could be mainly attributed to agglomeration of the clay particles. The variations in the ultimate strengths and initial moduli of the PI hybrid films with different clay contents are plotted in Figure 8. The elongation percentages required for breaking the hybrid fibers were all in the range of 2–3%. These values remained constant for increases in the organoclay loading in the range of 0.25–1.00 wt %. This result is characteristic of materials reinforced with stiff inorganic materials and is indicative of an intercalated morphology.

Collectively, these results indicate that the enhanced mechanical properties of the films containing organoclays were directly due to the reinforcement provided by the intercalation of PI in the clay galleries and by the dispersion of the clay particles in the polymer matrix. The improvements in the tensile mechanical properties also depended on the interactions between the PI molecules and the layered clay and on the rigidity of the clay layers.

TABLE III
Tensile Properties of the PI Nanocomposite Films

Organoclay (wt %)	Ultimate strength (MPa)	Initial modulus (GPa)	Elongation at break (%)
0 (pure PI)	62	2.78	3
0.25	70	2.79	3
0.50	74	3.89	3
0.75	36	2.86	2
1.00	36	2.87	2

Water vapor permeability

The water vapor permeability values for hybrid films with clay loadings of 0–1.00 wt % are summarized in Table IV. In general, the gas permeabilities of the hybrid films were lower than those of the pure PI film. This behavior could be attributed to the presence of a rigid platelet clay with a high aspect ratio in the polymer matrix.

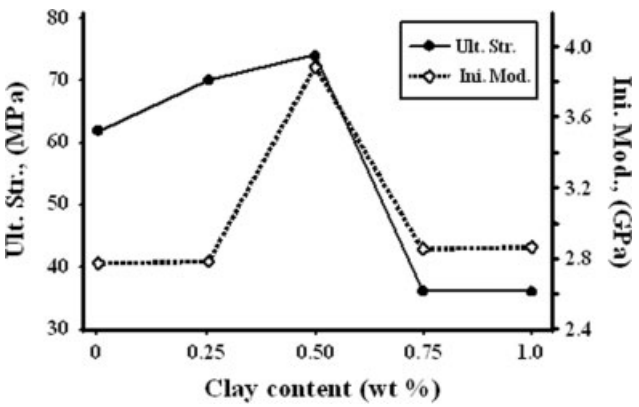

Figure 8 Effects of the clay loading on the ultimate strength and initial modulus of the PI hybrid films.

TABLE IV
Gas Permeabilities of the PI Nanocomposite Films

Organoclay (wt %)	Film thickness (μm)	MVTR [a] ($g/m^2/day$)	P_c/P_p [b]
0 (pure PI)	79	430	1.00
0.25	81	240	0.56
0.50	80	200	0.47
0.75	89	200	0.47
1.00	62	200	0.47

[a] Moisture vapor transmission rate.
[b] Composite permeability/polymer permeability (i.e., relative permeability rate).

The water vapor permeabilities calculated from the data are shown as relative permeabilities (composite permeability/polymer permeability). A 44% reduction in the permeability coefficient was observed from the pure PI film to the 0.25 wt % PI hybrid film. This lowering of the permeability in the hybrid was due to the presence of dispersed clay layers with large aspect ratios in the polymer matrix, as shown for other nanocomposites.[42,43] However, in comparison with other polymer hybrid films,[20,31,44] no significant changes in the water vapor permeability were observed in our systems. The water vapor permeability values of the PI hybrid films with various clay contents were found to be virtually unchanged from this value for organoclay loadings in the range of 0.50–1.00 wt %. This implied that varying the clay content did not result in improvements in the gas barrier of the PI matrix, as is evident in Table IV.

CONCLUSIONS

We prepared and characterized colorless PI/C_{12}PPh–mica nanocomposite films, using 6FDA and TFB in DMAc. XRD and electron microscopy studies indicated that the as-prepared PI hybrid films were nanocomposite materials. In addition, SEM and TEM studies confirmed that the organoclays were intercalated and revealed some agglomeration of the clay particles within the polymer matrix. The thermomechanical properties of the nanocomposites improved with an increasing organoclay loading up to a critical loading of 0.50 wt %. The water vapor permeability dropped markedly with the addition of 0.25 wt % organoclay but remained almost constant with a further increase in the clay loading. The results of electron microscopy analyses indicated that for clay loadings below 0.50 wt %, the clay particles were dispersed in the polymer matrix without substantial agglomeration. When the clay content was increased to 0.75 wt % and above, however, a denser agglomerated structure formed in the polymer matrix. For this hybrid system, the largest improvement in the thermomechanical properties was found for a C_{12}PPh–mica loading of only 0.50 wt %. Overall, these results show that the addition of a small amount of C_{12}PPh–mica is sufficient to improve the properties of a colorless PI.

References

1. Ando, S.; Sawada, T.; Inoue, Y. Electron Lett 1993, 29, 2143.
2. Mittal, K. L. Polyimides: Synthesis, Characterization, and Applications; Plenum: New York, 1984.
3. Feger, C.; Khojasteh, M. M.; Htoo, M. S. Advances in Polyimide Science and Technology; Technomic: Lancaster, PA, 1993.
4. So, Y. H.; Heeschen, J. P. J Org Chem 1997, 62, 3552.
5. Wolfe, J. F.; Arnold, F. E. Macromolecules 1981, 14, 909.
6. Qu, W.; Ko, T. Z.; Vora, R. H.; Chung, T. S. Polymer 2001, 42, 6393.
7. Yang, C. P.; Yang, H. W. U.S. Pat. 6,093,790 (2000).
8. St. Clair, A. K.; Slemp, W. S. SAMPE J 1985, 21, 28.
9. Myung, B. Y.; Kim, J. S.; Yoon, T. H. J Polym Sci Part A: Polym Chem 2003, 41, 3361.
10. Seino, H.; Mochizuki, A.; Haba, O.; Ueda, M. J Polym Sci Part A: Polym Chem 1998, 36, 2261.
11. Ree, M.; Shin, T. J.; Kim, S. I.; Woo, S. H.; Yoon, D. Y. Polymer 1998, 39, 2521.
12. Seino, H.; Haba, O.; Ueda, M.; Mochizuki, A. Polymer 1999, 40, 551.
13. Yang, C. P.; Chen, R. S.; Chen, K. H. J Polym Sci Part A: Polym Chem 2003, 41, 922.
14. Yang, C. P.; Sue, Y. Y. Polymer 2005, 46, 5778.
15. Lan, T.; Kaviratna, P. D.; Pinnavaia, T. J. Chem Mater 1995, 7, 2145.
16. Usuki, A.; Koiwai, A.; Kojima, Y.; Kawasumi, M.; Okada, A.; Kurauchi, T.; Kamigaito, O. J Appl Polym Sci 1995, 55, 119.
17. Galgali, G.; Ramesh, C.; Lele, A. Macromolecules 2001, 34, 852.
18. Osman, M. A.; Mittal, V.; Morbidelli, M.; Suter, U. W. Macromolecules 2003, 36, 9851.
19. Yeun, J.-H.; Bang, G.-S.; Park, B. J.; Ham, S. K.; Chang, J.-H. J Appl Polym Sci 2006, 101, 591.
20. Chang, J.-H.; Park, K. M.; Cho, D.; Yang, H. S.; Ihn, K. J. Polym Eng Sci 2001, 41, 1514.
21. Chang, J.-H.; Kim, S. J. Joo, Y. L.; Im, S. Polymer 2004, 45, 919.
22. Chang, J.-H.; Park, K. M. Eur Polym J 2000, 36, 2185.
23. Yano, K.; Usuki, A.; Okada, A.; Kurauchi, T.; Kamigaito, O. J Polym Sci Part A: Polym Chem 1993, 31, 2493.
24. Rogers, F. E. U.S. Pat. 3,356,648 (1964).
25. Li, F.; Fang, S.; Ge, J. J.; Honigfort, P. S.; Chen, J. C.; Harris, F. W.; Cheng, S. Z. D. Polymer 1999, 27, 5964.
26. Misra, A. C.; Tesoro, G.; Pendarkar, S. M. Polymer 1992, 33, 1078.
27. Chang, J.-H.; Park, D. K.; Ihn, K. J. J Appl Polym Sci 2002, 84, 2294.
28. Ma, S. L.; Kim, Y. S.; Lee, J. H.; Kim, J. S.; Kim, I.; Won, J. C. Polymer (Korea) 2005, 29, 204.
29. Hsiao, S. H.; Liou, G. S.; Chang, L. M. J Appl Polym Sci 2001, 80, 2067.
30. Ke, Y.; Lu, J.; Yi, X.; Zhao, J.; Qi, Z. J Appl Polym Sci 2000, 78, 808.
31. Yano, K.; Usuki, A.; Okada, A.; Kurauchi, T.; Kamigaito, O. J Polym Sci Part A: Polym Chem 1997, 35, 2289.
32. Vaia, R. A.; Jandt, K. D.; Kramer, E. J.; Giannelis, E. P. Chem Mater 1996, 8, 2628.
33. Dagani, R. Chem Eng News 1999, 77, 25.
34. Chang, J.-H.; Seo, B.-S.; Hwang, D.-H. Polymer 2002, 43, 2969.

35. Li, F.; Ge, J.; Honigfort, P.; Fang, S.; Chen, J. C.; Harris, F.; Cheng, S. Polymer 1999, 40, 4987.
36. Agag, A.; Takeichi, T. Polymer 2000, 41, 7083.
37. Fornes, T. D.; Yoon, P. J.; Hunter, D. L.; Keskkula, H.; Paul, D. R. Polymer 2000, 43, 5915.
38. Xu, H.; Kuo, S.-W.; Lee, J.-S.; Chang, F.-C. Macromolecules 2002, 35, 8788.
39. Haddad, T. S.; Lichtenhan, J. D. Macromolecules 1996, 29, 7302.
40. Chen, L.; Wong, S.-C.; Pisharath, S. J Appl Polym Sci 2003, 88, 3298.
41. Kojima, Y.; Usuki, A.; Kawasumi, M.; Okada, A.; Fukushima, Y.; Kurauchi, T.; Kamigaito, O. J Mater Res 1993, 8, 1185.
42. Gorrasi, G.; Tortora, M.; Vittoria, V.; Pollet, E.; Lepoittevin, B.; Alexandre, M.; Dubois, P. Polymer 2003, 44, 2271.
43. Bharadwaj, R. K. Macromolecules 2001, 34, 9189.
44. Kojima, Y.; Usuki, A.; Kawasumi, M.; Okada, A.; Kurauchi, T.; Kamigaito, O. J Appl Polym Sci 1994, 32, 625.